Applying optical coherence tomography for weld depth monitoring in remote laser welding of automotive battery tab connectors

Cite as: J. Laser Appl. **33**, 012028 (2021); https://doi.org/10.2351/7.0000336
Submitted: 30 November 2020 . Accepted: 30 November 2020 . Published Online: 29 December 2020

Mikhail Sokolov, Pasquale Franciosa, Tianzhu Sun, Dariusz Ceglarek, Vincenzo Dimatteo, Alessandro Ascari, Alessandro Fortunato, and Falk Nagel

Journal of Laser Applications ARTICLE scitation.org/journal/jla

Applying optical coherence tomography for weld depth monitoring in remote laser welding of automotive battery tab connectors

Cite as: J. Laser Appl. 33, 012028 (2021); doi: 10.2351/7.0000336
Submitted: 30 November 2020 · Accepted: 30 November 2020 ·
Published Online: 29 December 2020

Mikhail Sokolov,[1] Pasquale Franciosa,[1] Tianzhu Sun,[1] Dariusz Ceglarek,[1] Vincenzo Dimatteo,[2] Alessandro Ascari,[2] Alessandro Fortunato,[2] and Falk Nagel[3]

AFFILIATIONS

[1]WMG, University of Warwick, Coventry CV4 7AL, United Kingdom
[2]University of Bologna, Viale del Risorgimento 2, Bologna 40136, Italy
[3]Coherent (Deutschland) GmbH, Berzeliusstrasse 87, 22113 Hamburg, Germany

Note: Paper published as part of the special topic on Proceedings of the International Congress of Applications of Lasers & Electro-Optics 2020.

ABSTRACT

This paper addresses in-process monitoring of weld penetration depth (WPD) during remote laser welding of battery tab connectors using optical coherence tomography (OCT). The research aims at studying the impact of welding process parameters on the accuracy of WPD measurements. In general, the highest measurement accuracy is achievable by positioning the OCT measuring beam toward the bottom of the keyhole. However, finding and maintaining the alignment between the OCT measuring beam and the bottom of the keyhole is a challenging task because of the dynamic changes in the size and shape of the keyhole itself. The paper addresses the above challenge by (1) developing welding process parameters for the Al-Cu thin foil lap joint (Al 1050 foil 450 μm and Ni-plated Cu foil 300 μm) using a novel adjustable ring mode (ARM) laser and (2) integrating OCT technology with two beams: one targeting the bottom of the keyhole and another as a reference to the part surface (TwinTec technology). The methodology is underpinned by the "Keyhole Mapping" approach, which helps one to identify the optimal placement of the OCT measuring beam with considerations to both measurement accuracy and stability of the keyhole. Findings indicated that welding with the ARM laser results in a more stable process, reduces fluctuations of the keyhole opening, and, therefore, helps one to improve the measurement accuracy by a factor of 50% (from the average error of 0.22 mm to 0.11 mm). Results further identified that the feasible operating window of the OCT measuring beam, corresponding to the highest measurement accuracy, is below 20 μm in length.

Key words: remote laser welding, copper to aluminum welding, weld penetration depth, battery tab connectors, adjustable ring mode laser, optical coherence tomography

I. INTRODUCTION

There is a growing body of evidence on the impact of electric mobility on controlling emissions. Central to the entire strategy of environmental-friendly transport is the concept of switching from internal combustion engines to the electrical powertrain.[1] The electrical energy storage system is a dominant feature of this strategy as the battery is the most expensive and also the heaviest component of the electrical vehicle.[2] Recent studies show that the production of battery systems suffers from a number of technological challenges such as the increasing number of product variants and concepts conjugated with a lack of standardization for process and product design,[3] increased rejection rate,[4] and safety hazards from defective products.[5] Therefore, manufacturing systems are faced with the challenge of adapting to high volume production, new designs, and satisfying quality targets in a timely manner.[6] Failures induced by uncontrolled weld quality have two major downsides: (1) battery damage, i.e., uncontrolled weld penetration poses the

risk of the piercing of the battery cell, with subsequent leaking of harmful gases and fire and (2) scrapping of the whole battery pack as even one single defective weld if left undetected can cause the whole battery pack to malfunction (i.e., voltage drop).[7] This underscores the need for new technological solutions for welding of battery tab connectors and in-process monitoring of the weld quality along with corrective and/or preventive actions in order to achieve zero scrap.

With regard to welding technology, there is a growing interest in applying remote laser welding (RLW) in battery manufacturing due to several advantages such as single sided noncontact access, reduced and controlled heat input, and reduced processing time, with the possibility of making a single weld in a fraction of a second, thereby enabling high throughput necessary for the high vehicle production volume.[8] As such, RLW has already been successfully developed for applications involving aluminum or steel structures.[9] However, when it comes to dissimilar metal welding, as for any other thermal-fusion process, the main technical challenges are related to the control of intermetallic compounds (IMCs) and mitigation of cracking mechanisms. In fact, welding of dissimilar metals with laser technology involves significant mixing of two materials with different thermal and mechanical properties, which can lead to segregation and precipitates, poor compatibility and miscibility, and brittle intermetallic phases.[10,11] A previous study[12] concluded that the principle behind the formation of IMCs and weld cracking is related to the control of (1) heat input, (2) pick temperature in the molten pool, and (3) thermal cycles (preheating and postheating). Recently, few promising technological solutions have been developed for the control of IMCs and cracking mechanisms. They include laser beam oscillation, continuous wave (CW) and pulsed lasers, and infrared and visible lasers (both green and blue).[13,14] Coherent Inc. introduced a new concept of laser welding called the adjustable ring mode (ARM) laser.[15] The ARM laser provides independent control of power distribution in the inner core laser beam and outer ring-shaped laser beam. The inner core promotes the generation of the keyhole, while the ring-shaped laser beam allows controlling the distribution of temperature and cooling rate in and around the molten pool. Research has confirmed a positive effect of the ARM laser on keyhole stabilization.[16] The stability of the keyhole and, therefore, of the welding process is a vital indicator of the weld quality in those applications where partial penetration is required, such as welding of battery tab connectors. However, the application of ARM laser to welding of thin foil dissimilar metals remains an unexplored area of research and will be addressed in this paper. In terms of in-process monitoring of the weld quality, the recently introduced optical coherence tomography (OCT) allows the direct and in-process measurement of the keyhole depth. Assuming that the molten layer just underneath the keyhole bottom is negligible, the OCT sensor allows the direct measurement of the weld penetration depth (WPD).[17] With OCT, the laser light of a low coherent emitter is split into two beams: one propagates into the reference path ("reference beam") and the second beam, named "measuring beam," propagates through the welding head into the keyhole. The difference between the two light paths leads to an interference pattern and the distance data are extracted from the frequency of the occurring interference on the photo-detector.[18] Dorsch *et al.*[19] showed that the OCT measuring beam has to be accurately positioned with respect to the bottom of the keyhole; however, finding and maintaining the alignment between the OCT measuring beam and the bottom of the keyhole is a challenging task because of the dynamic changes in the size and shape of the keyhole.[20] Those changes affect the measurement error, which, in general, depends upon multiple sources of variations. Variations are grouped into several categories: "mechanical," "material," "optical," and "process." The "mechanical variation" originates from those variations related to clamping or part-to-part gap and surface waviness. Variations in the material thickness or material properties can be categorized as "material variation." The "optical variation" includes, for example, variations in the refraction index in the plasma plume above the molten pool, which results in fluctuations of the laser absorbed by the material, and potential chromatic aberration caused by the interaction of the OCT measuring beam and process laser beam passing through the same lens. The "process variation" is caused by variations of the welding process parameters, which have a direct impact on the physics of the keyhole formation and the melt pool dynamics. Research conducted in Ref. 21 concluded that the cumulative effect of those variations leads to the fact that the position of the OCT measuring beam is not universal and has to be adjusted for every specific welding setup. This paper aims at studying the impact of process variation on the WPD measurements during RLW of the Al-Cu thin foil lap joint (Al 1050 foil 450 μm and Ni-plated Cu foil 300 μm) using OCT technology in conjunction with the ARM laser. It builds upon the "Keyhole Mapping" approach,[21] which focused on finding the optimal position of the OCT measuring beam and was tested for the fillet lap joint configuration of similar Al-Al sheet metal parts. The extension of this work to dissimilar metal welding of thin foil Al and Cu components brings the following technical challenges, which will be discussed throughout the paper:

(1) *Low measurement accuracy*: process variation generates fluctuations of the keyhole and unwanted multiple reflections from the keyhole wall, which must be analyzed and filtered, in order to ensure that the measurement accuracy is at least five times higher than the thickness of the welded parts. This is necessary to assure that the control of the WPD is within predefined limits, hence, to avoid full penetration or lack of bonding between the foils;
(2) *Dynamic changes of size and shape of the keyhole*: the measurement of the keyhole has shown significantly different shapes and sizes, i.e., a conical geometry of the keyhole in aluminum and bottle-shaped geometry in copper alloys;[22–24] and
(3) *Position of the OCT measuring beam*: the measurement accuracy relies upon the position of the OCT measuring beam—the highest measurement accuracy is achievable by positioning the OCT measuring beam as close as possible to the bottom of the keyhole.

II. MATERIALS AND METHODS

A. Experimental configuration and setup

The experiments were conducted using aluminum 1050 450 μm and nickel-plated copper foil 300 μm, which were welded

by the CW multimode Coherent fiber laser HighLight FL-ARM 10 000. The conceptual arrangement of the ARM beam and OCT measuring beam is illustrated in Figs. 1(a) and 1(b). Figure 1(c) shows the measured power distribution (false color plot) of the ARM beam obtained with the focus meter (Primes GmbH, Germany). The ARM beam was delivered through the WeldMaster Scan&Track remote welding head (YW52 Precitec GmbH, Germany). All experiments were performed without shielding gas and without filler wire. Samples were wiped with acetone before welding to remove surface contaminations. In order to confirm the results of the OCT signals, high speed filming was performed with Photron FASTCAM NOVA S6 and CAVILUX Smartlaser illumination (808 nm with exposure of 20 μs and fps of 40 000). Figure 2 shows the experimental setup, and details of the equipment are in Tables I and II.

The IDM (In-process Depth Meter, Precitec GmbH, Germany) was used as a OCT sensor and was installed just below the motorized collimator of the welding head WeldMaster Scan&Track. This allows one to defocus the ARM beam independently of the OCT measuring beam. However, the OCT measuring beam was deflected and focused using the same motorized mirror and focusing unit of the welding head. The coordinate system (x, y), which defines the position of the OCT measuring beam, was inside the IDM collimator.

The position of the OCT measuring beam was controlled by manually adjusting the beam deflector on the IDM collimator.

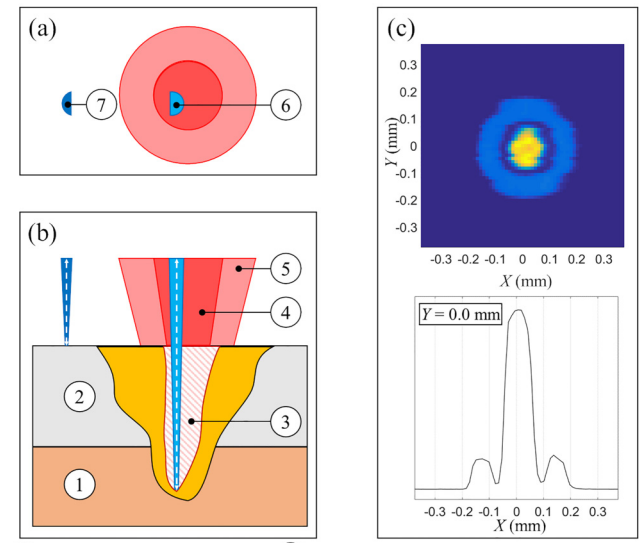

FIG. 1. (a) Top view of the ARM beam and OCT measuring beam. (b) Front view with the representation of the keyhole. (c) Measured power distribution (false color) of the ARM beam on focus (Primes GmbH).

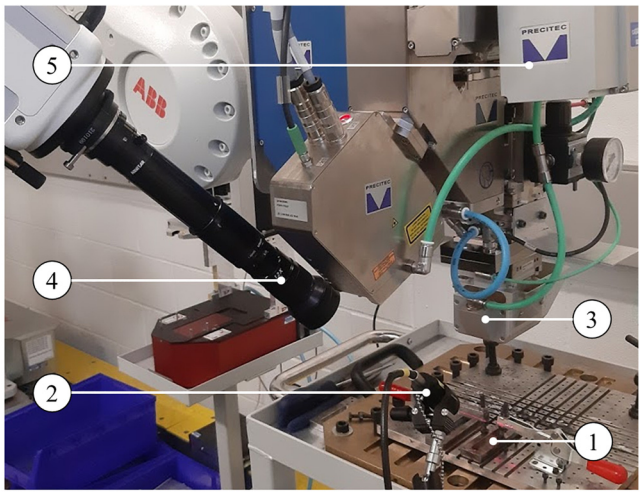

1 Clamping setup
2 CAVILUX Smartlaser illumination
3 WeldMaster Scan&Track
4 Photron FASTCAM NOVA S6
5 IDM sensor

FIG. 2. Experimental setup developed for collecting both OCT signals and high-speed images.

The IDM sensor was also equipped with the TwinTec module (Precitec GmbH, Germany), which allows one to split the OCT measuring beam into two sub-beams (see Fig. 1): the first one tracks the material surface ("OCT measuring beam—surface"), whereas the second beam ("OCT measuring beam—keyhole") is aligned to the bottom of the keyhole. As the TwinTec module uses a prism to refract a section of the OCT measuring beam, the resulting spot is a segment of a circle. The additional distance traveled by the "OCT measuring beam—surface" is approximately 150 μm, which needs to be considered when processing the OCT signal. The effective keyhole depth is then obtained using the difference in distance traveled between the two OCT sub-beams.[25] The "OCT measuring beam—surface" is used to reduce the spread in the OCT

TABLE I. Specification of the welding setup.

HighLight FL-ARM	Units	Core	Ring
Nominal output power	W	5000	5000
Optical fiber diameter	μm	70	180
Spot diameter at focus	mm	0.14	0.36
Collimating length	mm	150	
Focusing length	mm	300	
Emission wavelength	nm	1080	

TABLE II. Specification of the OCT sensor setup.

IDM and TwinTec	Units	Value
Sampling rate	kHz	70
Emission wavelength	Nm	1550
Sensor beam max power	mW	10
Sensor beam intensity	%	30
Spot diameter	mm	0.05
Max measurement range	mm	10
TwinTec split intensity	%	50

signals as it compensates for the effect of the part surface waviness and other "mechanical variations."

B. Design of experiments and signal processing

The experiments were conducted in two sets: (i) selection and optimization of welding process parameters for the Al-Cu thin foil lap joint and (ii) investigation of the OCT sensor capability for monitoring of WPD.

The experimental plan for the first set (i) was divided into two setups: ID 1—"core + ring" (dual-beam welding) uses the combined power of both the ARM core and ring beams with varying power levels for the ring and fixed core power at 650 W and ID 2—"core-only" (single-beam welding) uses the power of the ARM core beam, while the ARM ring beam is off.

The second set (ii) of experiments was conducted with the welding parameters developed in set (i). OCT data were processed through the "keyhole mapping" approach. The keyhole mapping is obtained by linking the relative position of the OCT measuring beam, defined by x and y coordinates. Once OCT data, D_{OCT}, are collected for the given position of the OCT measuring beam [as shown in Fig. 3(a)], key signal features are extracted as listed below. The keyhole mapping approach uses a moving window that scans the whole signal. For each position of the moving window, the data points are processed by the kernel density estimation (KDE) as shown in Fig. 3(b). The extracted key signal features are (full description of the method can be found in Ref. [21]:

- *Interquartile range*, $P_{W,Q3}$–$P_{W,Q1}$, corresponds to 75% ($P_{W,Q3}$) and 25% ($P_{W,Q1}$) of the probability density function (PDF). Interquartile range is used to measure of the OCT signal spread and, therefore, to detect the start and end of the keyhole.
- *Measured WPD*, $P_{W,Q}$. A previous study[21] evaluated the sensitivity of the percentile on the accuracy of the output OCT signal and showed that the 80th percentile results in the highest accuracy, i.e., minimal deviation between $P_{W,Q}$ and the actual penetration depth, $P_{W,C}$, as measured by the metallographic analysis of cross sections.
- *Normalized modality index*, $P_{W,M}$, is computed using the Hartigans' dip test,[26] which measures the probability of observing a single-modal distribution of the PDF. The shape of the density function is a key feature that gives insights into the shape of the keyhole. Higher values of $P_{W,M}$ correspond to higher probability of obtaining single-modal distribution. Higher values of the normalized modality index are expected when the OCT measuring beam is positioned closer to the bottom of the keyhole.[21]

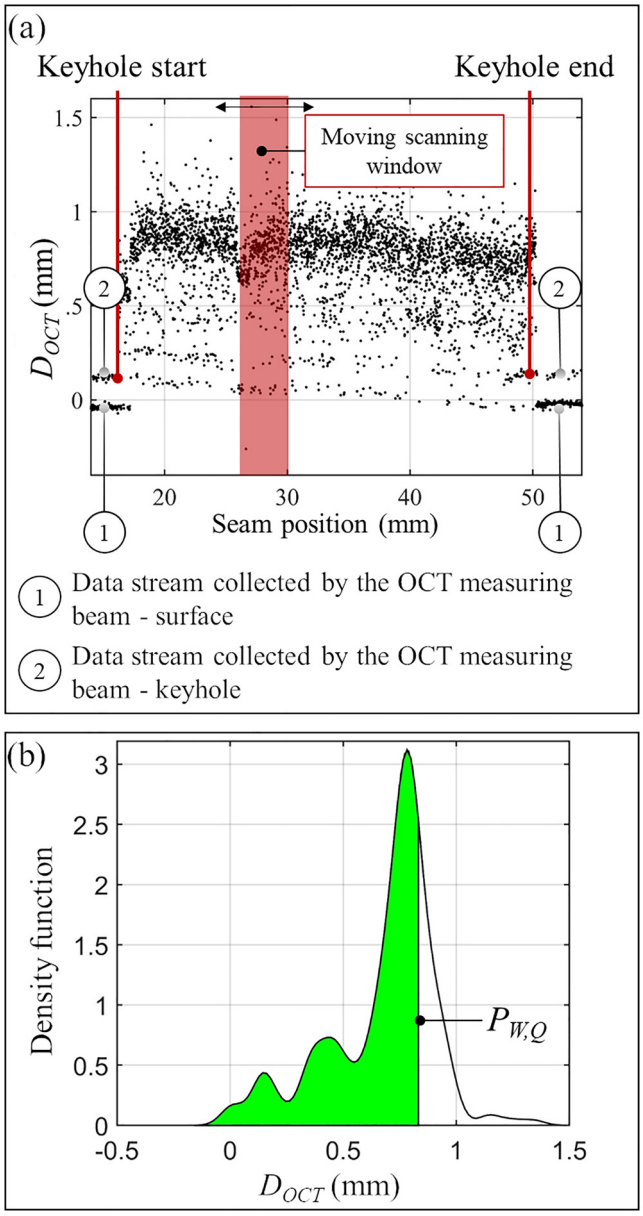

FIG. 3. (a) Example of the raw OCT signal; (b) density function of the data points belonging to the moving scanning window shown in (a) and computed using kernel density estimation (KDE).

The measurement accuracy of the OCT signal is quantified through the average WPD error, ε, which is the difference between the measured WPD, $P_{W,Q}$, and the average of the actual penetration depth, measured with metallographic analysis, $P_{W,C}$.

III. RESULTS AND DISCUSSION

A. Experimental set (i): Weld geometry optimization

Weld geometry has been optimized at the fixed welding speed of 175 mm/s in a linear welding pattern without beam oscillation. A total of 42 experiments were performed: 28 experiments with varying power of the ARM ring beam (50–1500 W) and with fixed power of the ARM core beam at 650 W (ID 1)—the selected core power was experimentally demonstrated to be the minimum level required to fully penetrate the upper Al plate (450 μm thickness), and 14 experiments with varying power at the ARM core beam (650–1000 W) and no power to the ARM ring beam (ID 2).

The results are shown in Fig. 4. The selection of process parameters to obtain optimized weld geometry was driven by the joint strength. The effective weld width (W_E) was measured at the interface between the two sheets, while the $P_{W,C}$ was measured as the depth into the lower sheet from the top sheet. Prescreening tests and tensile test results confirmed that W_E of ~0.4 mm and $P_{W,C}$ of ~0.7 mm are sufficient to give 25 N/mm joint strength.[10] Within the selected optimal process window, W_E does not change much for both setups. Further increase in W_E and $P_{W,C}$ leads to the brittle fracture of the joint due to the increased distribution of brittle intermetallic compounds (i.e., more Cu mixed to Al). Table III summarizes the optimized welding parameters for the two setups.

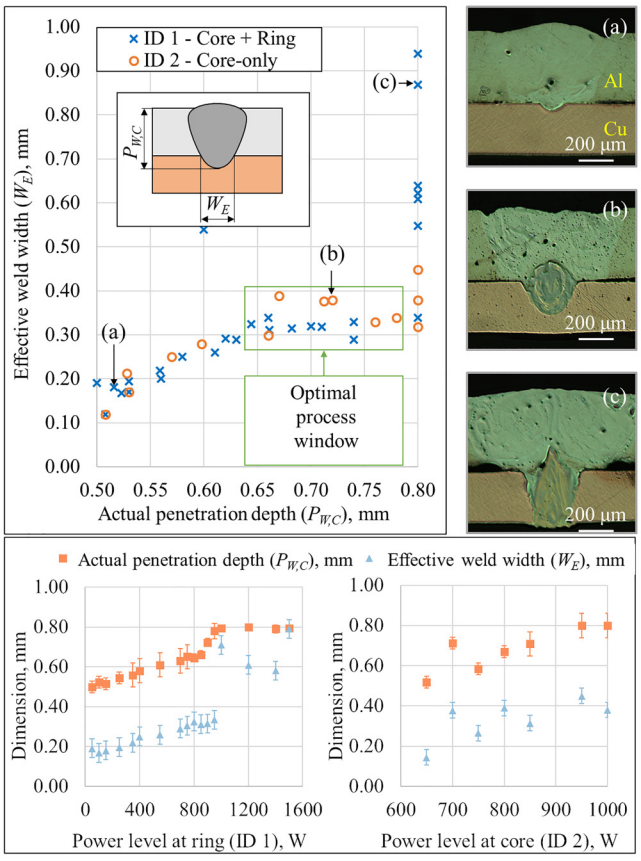

FIG. 4. Experimental set (i): mean values with 1-sigma error bars (bottom) and combined plot (top). (a) No connection between Al and Cu. (b) optimized weld geometry. (c) full penetration with wide weld but brittle structure.

B. Experimental set (ii): Keyhole mapping

Two types of OCT signals have been introduced: "Distinct OCT Signal" and "Indistinct OCT Signals." "Distinct OCT Signal" refers to those OCT signals that meet two criteria:

- Criterion (1)—average WPD error, ε, below 0.15 mm in order to keep WPD within the limits of the optimal process window;
- Criterion (2)—normalized modality index, $P_{W,M}$, higher than 0.3 in order to guarantee single-mode distribution of the signal's PDF. This criterion allows one to discard those measurements generated by the OCT measuring beam not accurately positioned closer to the bottom of the keyhole yet exhibiting the low average WPD error.

"Indistinct OCT Signal" corresponds to those measurements that fail to satisfy criterion (1) or (2).

The keyhole mapping determines the position of the OCT measuring beam whose signals fulfill criteria (1) and (2). The analysis has been conducted for the optimized process parameters shown in Table III. Figure 5(a) shows the tested positions of the OCT measuring beam in relation to the ARM core spot, for setup ID 1 ("core + ring"). Figure 5(c) shows a typical case with the bimodal distribution of the OCT signal's PDF and classified as "Indistinct OCT Signal." This signal has been generated by the OCT measuring beam outside the bottom of the keyhole, as indicated by the bimodal shape of the PDF and measured by the normalized modality index ($P_{W,M} = 0.066$).

The position of the OCT measuring beam, with $x = 2.31$ mm and $y = 1.61$ mm, fulfills both criteria for ID 1 and ID 2. It is interesting to notice that the operating window of the OCT measuring beam was only limited to 20 μm in x and less than 10 μm in y for setup ID 1. However, for ID 2, the window became even narrower in both x and y and below 10 μm in length. This behavior is explained by presumably wider keyhole in ID 1 comparing to ID 2 due to the effect of the ARM ring beam.

TABLE III. Optimized process parameters and actual penetration depth.

Setup	ID 1 (core + ring)	ID 2 (core-only)
Welding speed	175 mm/s	175 mm/s
Focal point offset	0 mm	0 mm
Power ARM core	650 W	800 W
Power ARM ring	900 W	0 W
$P_{W,C}$	0.78 ± 0.02 mm	0.68 ± 0.03 mm
Representative cross section	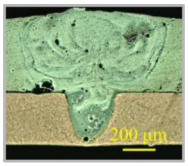	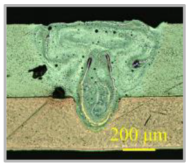

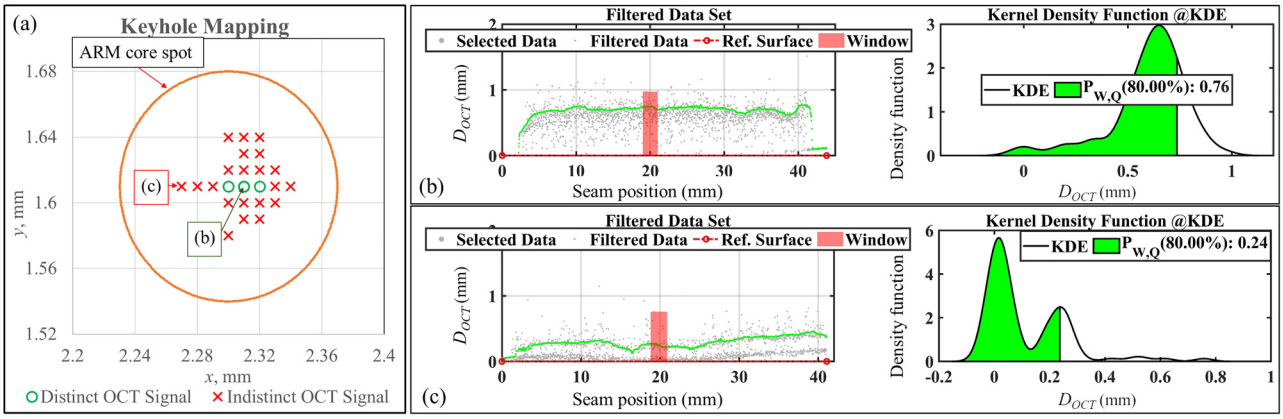

FIG. 5. (a) Keyhole mapping for ID 1 and "TwinTec off." (b) "Distinct OCT signal" shown as green dot: $P_{W,Q} = 0.76$; $P_{W,M} = 0.986$; $\varepsilon = 0.02$. (c) "Indistinct OCT signal" shown as red cross: $P_{W,Q} = 0.24$; $P_{W,M} = 0.066$; $\varepsilon = 0.56$ ($P_{W,C}$ for ID 1 = 0.78 ± 0.02).

C. Signal processing

In order to quantify the impact of welding parameters on the measurement accuracy, the OCT signals were processed for both optimized ID 1 and ID 2 (Table III) in two configurations: "TwinTec on" using both "surface" and "keyhole" sub-beams of the OCT measuring beam and "TwinTec off" with the "surface" sub-beam turned off. For each setup, five replications were performed, with the same welding parameters, and in each experiment 10 moving windows were chosen to extract the key features of the OCT signal as explained in the method description. Data have been processed with one-way ANOVA, with a confidence value of 0.1.

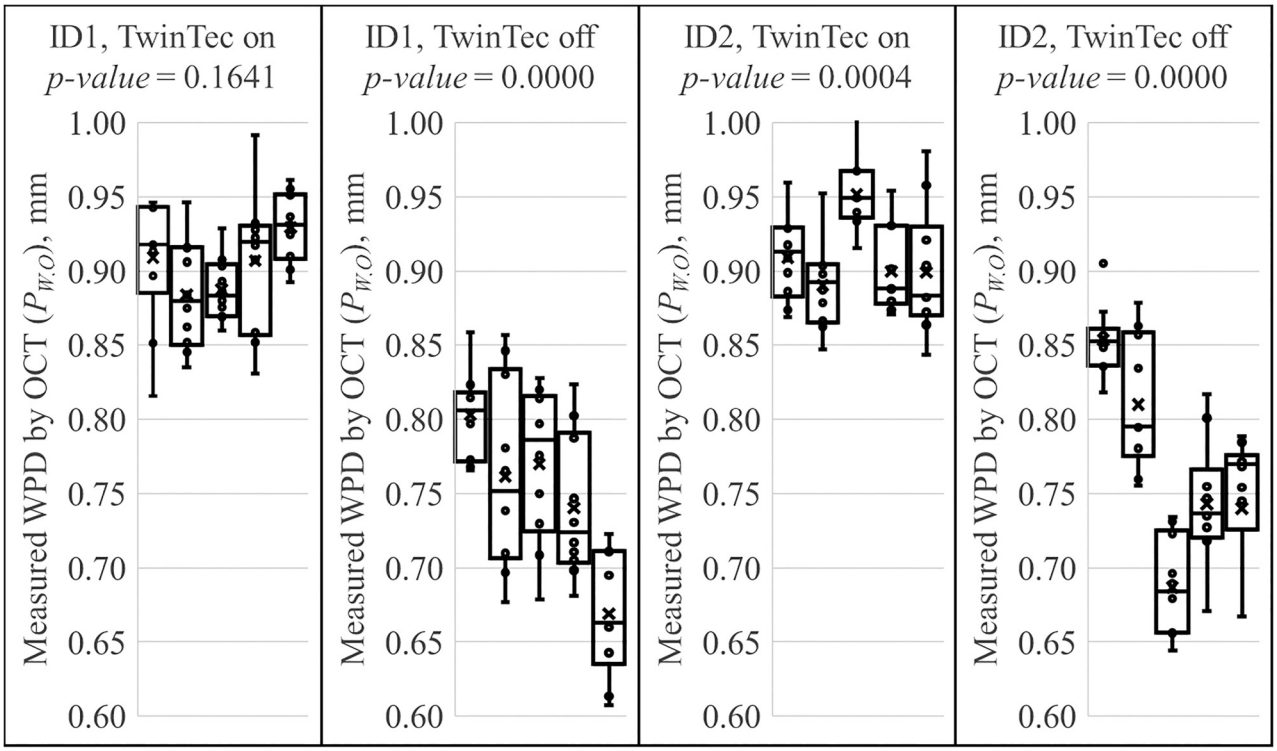

FIG. 6. Repeatability study for ID 1 and ID 2 with "TwinTec on" and "TwinTec off"——five weld replications ($P_{W,C}$ for ID 1 = 0.78 ± 0.02; $P_{W,C}$ for ID 2 = 0.68 ± 0.03).

Results are shown in Fig. 6, testing the hypothesis that the samples within the setup are having the same mean against the alternative hypothesis that means are not all the same; if p-value is higher than 0.1, the hypothesis is accepted. The p-value is rounded to four decimal places.

The effect of TwinTec is discussed as follows:

- *TwinTec on*—The obtained results indicate that the measured WPD statistically varies in setup ID 2 (with p-value of 0.0004), which translates to the fact that the OCT signals are statistically not repeatable. This may be caused by the fast fluctuations in the keyhole opening as a result of the welding parameters only ARM core beam and no ring beam. Conversely, in setup ID 1, p-value of 0.1641 suggests that the OCT signal is statistically repeatable for five replications.
- *TwinTec off*—both setups with TwinTec off show low p-value close to zero, indicating high variability in repeated welds. This could be imputed to mechanical variations, such as sample misalignment and surface waviness.

In order to confirm those results, high speed filming was performed. Figures 7(a) and 7(b) show a few consecutive frames of ID 1 and ID 2, respectively. The combination of the ARM core and ring beams (ID 1) produces a smoother process with a significant reduction in spatters (high speed videos could be watched online: https://www.youtube.com/watch?v=IOjx400wMQw).

This eventually translates to increased stability of the keyhole which tends to stay open longer. The box-plot in Fig. 7(c) shows that the OCT signal measured during weld configuration ID 1 and "TwinTec on" exhibits significantly lower average WPD error (0.11 mm), compared to ID 2 and "TwinTec on" (0.22 mm). It is interesting to notice though that on average the WPD error is significantly lower (below 0.1 mm) for both setups ID 1 and ID 2 when the TwinTec is turned off. Nevertheless, as already shown in the repeatability study in Fig. 6, the spread in the $P_{W,Q}$ is significantly high for "TwinTec off."

The present results are significant in two major respects. First, the combination of the ARM core and ring beams (ID 1) helps one to produce more repeatable welds with reduced spatters that result in the increased stability of the keyhole itself. As a consequence, the OCT signal shows repeatable data compared to the case with the ring beam turned off (ID 2). It is interesting to notice that though the average values of the actual penetration depths are significantly different for the two setups ($P_{W,C}$ for ID 1 = 0.78; $P_{W,C}$ for ID 2 = 0.68), the average value of $P_{W,Q}$ for ID 2 is about 0.9 mm, which is comparable to the one obtained for ID 1. This phenomenon may be imputed to the shape of the keyhole, which changes between ID 1 and ID 2, causing multiple reflections inside the keyhole, and, therefore, increasing the traveled distance of the OCT measuring beam.

Second, when the TwinTec is off, the OCT signal is statistically not repeatable with high spread of $P_{W,Q}$ and $P_{W,M}$ as shown in Figs. 7(c) and 7(d).

However, this phenomenon is clearly not caused by the welding process itself but rather by the approach used to process the OCT data and extract the key features. For instance, when the TwinTec is off, the OCT data are aligned to an approximated

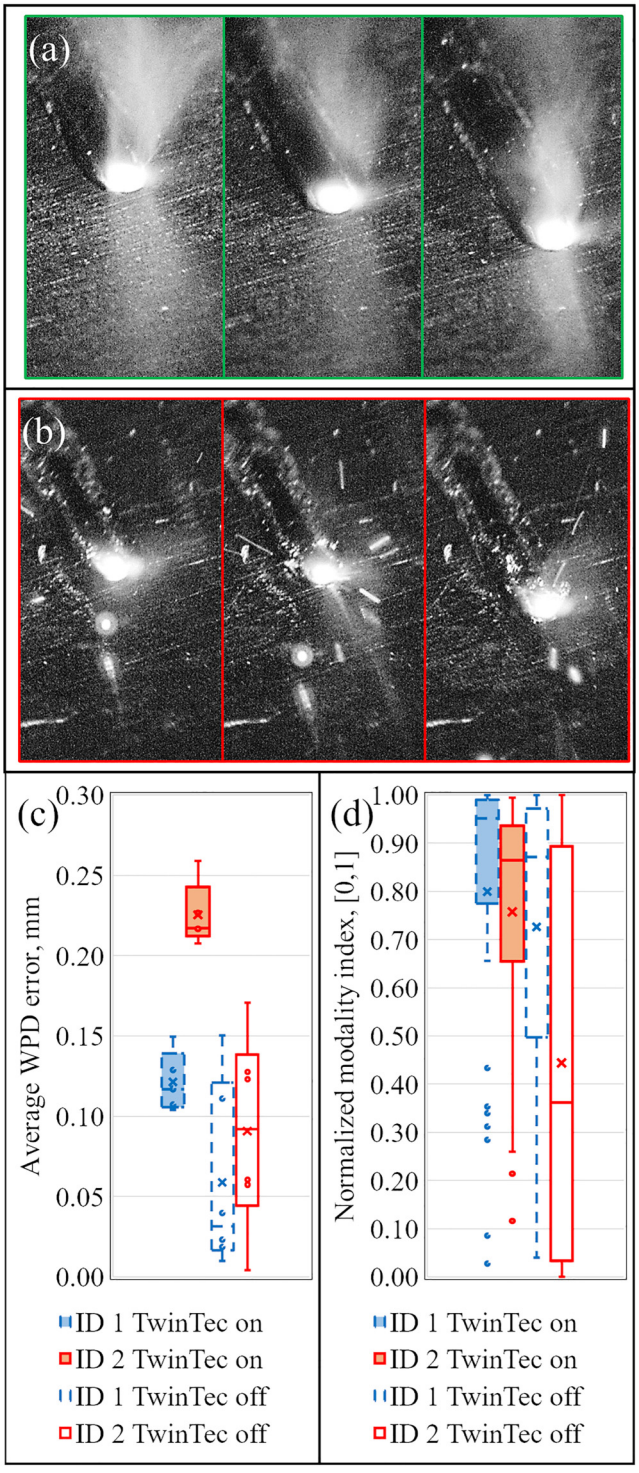

FIG. 7. Few consecutive frames grabbed during high speed filming for (a) ID 1 and (b) ID 2. Box-plot of (c) average of WPD error and (d) normalized modality using 10 moving windows.

reference surface that best fits the data points belonging to the part surface just before the keyhole starts, as shown in Fig. 3(a). The result of the best fitting approach clearly depends on few sources of variations, such as part misalignment and surface waviness. In the case of thin foil welding those variations are significant considering also the induced thermal deformation which further affects the part surface prior welding. Those variations are compensated when the TwinTec is turned on, since the reference surface is directly measured by the "OCT measuring beam—surface." Moreover, the increase, on average, of the WPD error for "TwinTec on," compared to "TwinTec off," is attributed to the fact that the measured WPD is calculated using the difference in the traveled distance between OCT sub-beams ("OCT measuring beam—surface" and "OCT measuring beam—keyhole"). In this approach, we have estimated from the data that the additional distance traveled by the "OCT measuring beam—surface" is approximately 150 μm. However, no repeatability study has been carried out to confirm this finding. Future experiments, using a broader range of controlled mechanical variations,[27] could shed more light on the effects of the welding setup and possible compensations of those by the use of "OCT measuring beam—surface."

IV. CONCLUSIONS AND FINAL REMARKS

This paper investigated the capability of OCT technology for in-process monitoring of weld penetration depth during remote laser welding of thin foil Al and Cu components used in automotive battery tab connectors. The critical defects can be determined by too large WPD causing heat damage of the battery cell or too small WPD resulting in no electrical connection. Both scenarios may cause scrapping the whole battery unit.

We have concluded that TwinTec technology is essential to produce repeatable data and compensate mechanical variations such as part misalignment and surface waviness and to overcome the issues faced in approximating the reference surface when the TwinTec is turned off. Furthermore, ARM laser technology has shown significant improvement to the weld quality and welding process stability. Key findings are discussed as follows:

- *Measurement accuracy of WPD*. The application of ARM laser with independent control of the laser power on both core and ring beams allows one to reduce the average WPD error and increase OCT measurement accuracy of about 50%: from 0.22 mm with only ARM core beam (single-beam welding) to 0.11 mm in the case of the combined ARM core and ring beams (dual-beam welding). The improved accuracy of the WPD measurement in battery tab connectors allows one to exclude the potential battery cell penetration or lack of connection between the foils and contributed in developing the necessary step to enable closed-loop weld penetration depth control using OCT for RLW of dissimilar metals.
- *Size and shape of the keyhole*. Findings also highlight the importance of keyhole stability for accurate WPD monitoring as the OCT signal is unstable due to fast fluctuations of the keyhole opening during single-beam welding. The synergy of the ARM core and ring beams (dual-beam welding) influenced the process stability in a very positive way: high-speed camera observation of the weld and OCT signal analysis confirmed increased stability of the keyhole.
- *Position of the OCT measuring beam*: The accuracy of WPD strongly depends on the precise positioning of the OCT measuring beam. The experimental results have identified a very narrow feasible operating window of the OCT measuring beam (20 μm in the best case with ARM ring beam) where distinct WPD measurement is achieved. Moreover, the signals received outside the bottom of the keyhole, as indicated by the shape of the PDF and measured by the modality index, is a key feature and provide important insights about the dynamics and shape of the keyhole.

Further research should be undertaken to investigate the possibility to better decouple the two data streams ("surface" and "keyhole") generated by TwinTec technology, hence, to reduce signal biasing. An important issue to consider for future research is the automation of keyhole mapping and, therefore, the fast and accurate detection of the optimal placement of the OCT measuring beam. A possible solution can be the integration of a double motorized collimator that will allow communication with the controller of the welding head, enabling closed-loop weld penetration depth control. Furthermore, the impact of additional sources of variations, such as part-to-part gap, focal offset, and welding speed, will be investigated in future works.

ACKNOWLEDGMENTS

This study was partially supported by (1) WMG HVM Catapult; (2) APC UK project: Chamaeleon—New Lightweight Materials and Processing Technologies for Common Lightweight Architecture of Electric and Hybrid Powertrain Systems; and (3) Innovate UK IDP15 project LIBERATE: Lightweight Innovative Battery Enclosures using Recycled Aluminium Technologies. The authors greatly acknowledge the technical support of Coherent during the welding trials.

NOMENCLATURE

D_{OCT}	= Distance measured by OCT, mm
$P_{W,C}$	= Actual penetration depth by cross section, mm
$P_{W,M}$	= Normalized modality index, [0,1]
$P_{W,Q}$	= Measured WPD by OCT, mm
W_E	= Effective weld width, mm
x, y	= Position of the OCT measuring beam, mm

Greek

ε	= Average WPD error, mm

REFERENCES

[1]N. Rietmann and T. Lieven, "How policy measures succeeded to promote electric mobility—Worldwide review and outlook," J. Cleaner Prod. **206**, 66–75 (2019).
[2]M. Horn, J. MacLeod, M. Liu, J. Webb, and N. Motta, "Supercapacitors: A new source of power for electric cars?" Econ Anal Policy **61**, 93–103 (2019).
[3]M. K. Chinnathai, B. Alkan, D. Vera, and R. Harrison, "Pilot to full-scale production: A battery module assembly case study," Proc. CIRP **7**, 796–801 (2018).
[4]A. Kölmel, A. Sauer, and G. Lanza, "Quality-oriented production planning of battery assembly systems for electric mobility," Proc. CIRP **23**, 149–154 (2014).

[5]G. J. Offer, D. Howey, M. Contestabile, R. Clague, and N. P. Brandon, "Comparative analysis of battery electric, hydrogen fuel cell and hybrid vehicles in a future sustainable road transport system," Energy Policy **38**, 24–29 (2010).
[6]L. Seybold, M. Witczak, P. Majdzik, and R. Stetter, "Towards robust predictive fault-tolerant control for a battery assembly system," Int. J. Appl. Math. Comput. Sci. **25**, 849–862 (2015).
[7]A. Das, I. Butterworth, I. Masters, and D. Williams, "Microstructure and mechanical properties of gap-bridged remote laser welded (RLW) automotive grade AA 5182 joints," Mater. Charact. **145**, 697–712 (2018).
[8]P. Franciosa, M. Sokolov, S. Sinha, T. Sun, and D. Ceglarek, "Deep learning enhanced digital twin for closed-loop in-process quality improvement," CIRP Ann. **69**, 369–372 (2020).
[9]D. Ceglarek, *et al.*, "Rapid deployment of remote laser welding processes in automotive assembly systems," Ann. CIRP **64**(1), 389–394 (2015).
[10]V. Dimatteo, A. Alessandro, and F. Alessandro, "Continuous laser welding with spatial beam oscillation of dissimilar thin sheet materials (Al-Cu and Cu-Al): Process optimization and characterization," J. Manuf. Process. **44**, 158–165 (2019).
[11]A. Ascari, A. Fortunato, and V. Dimatteo, "Short pulse laser welding of aluminum and copper alloys in dissimilar configuration," J. Laser Appl. **32**, 022025 (2020).
[12]H. R. Kotadia, P. Franciosa, and D. Ceglarek, "Challenges and opportunities in remote laser welding of steel to aluminium," MATEC Web Conf. **269**, 02012 (2019).
[13]H. Pantsar, E. Dold, J. Gabzdyl, E. Kaiser, T. Hesse, M. Kirchhoff, and B. Faisst, "New welding techniques and laser sources for battery welding," *Proc. SPIE* 10525, 105250E (2018).
[14]J. P. Feve, M. S. Sa, M. Finuf, R. Fritz, J. M. Pelaprat, and M. Zediker, "500 watt blue laser system for welding applications," *Proc. SPIE* 10900, 1090004 (2019).
[15]M. R. Maina, Y. Okamoto, A. Okada, M. Närhi, J. Kangastupa, and J. Vihinen, "High surface quality welding of aluminum using adjustable ring-mode fiber laser," J. Mater. Process. Technol. **258**, 180–188 (2018).
[16]L. Wang, M. Mohammadpour, B. Yang, X. Gao, J.-P. Lavoie, K. Kleine, F. Kong, and R. Kovacevic, "Monitoring of keyhole entrance and molten pool with quality analysis during adjustable ring mode laser welding," Appl. Opt. **59**, 1576–1584 (2020).
[17]T. Bautze and M. Kogel-Hollacher, "Keyhole depth is just a distance: The IDM sensor improves laser welding processes," Laser Technik J. **11**, 39–43 (2014).
[18]P. J. Webster, L. G. Wright, K. D. Mortimer, B. Y. Leung, J. X. Yu, and J. M. Fraser, "Automatic real-time guidance of laser machining with inline coherent imaging," J. Laser Appl. **23**, 022001 (2011).
[19]F. Dorsch, W. Dubitzky, L. Effing, P. Haug, J. Hermani, and S. Plasswich, "Capillary depth measurement for process control," *Proc. SPIE* 10097, 1009708 (2017).
[20]M. Boley, F. Fetzer, R. Weber, and T. Graf, "Statistical evaluation method to determine the laser welding depth by optical coherence tomography," Opt. Lasers Eng. **119**, 56–64 (2019).
[21]M. Sokolov, P. Franciosa, R. Al Botros, and D. Ceglarek, " Keyhole mapping to enable closed-loop weld penetration depth control for remote laser welding of aluminium components using optical coherence tomography," J. Laser Appl. **32**, 032004 (2020).
[22]B. J. Aalderink, D. F. de Lange, R. G. K. Aarts, and J. Meijer, " Keyhole shapes during laser welding of thin metal sheets," J. Phys. D Appl. Phys. **40**, 5388–5393 (2007).
[23]M. Schmoeller, C. Stadter, S. Liebl, and M. F. Zaeh, "Inline weld depth measurement for high brilliance laser beam sources using optical coherence tomography," J. Laser Appl. **31**, 022409 (2019).
[24]C. Stadter, M. Schmoeller, L. von Rhein, and M. F. Zaeh, " Real-time prediction of quality characteristics in laser beam welding using optical coherence tomography and machine learning," J. Laser Appl. **32**, 022046 (2020).
[25]M. Kogel-Hollacher, M. Schoenleber, T. Bautze, M. Strebel, and R. Moser, "Measurement and Closed-Loop Control of the Penetration Depth in Laser Materials Processing," in *9th International Conference on Photonic Technologies LANE, Fürth, Germany, 19–22 September 2016* (Elsevier Procedia, 2016).
[26]J. A. Hartigan and P. M. Hartigan, "The dip test of unimodality," Ann. Stat. **13**, 70–84 (1985).
[27]P. Franciosa, A. Serino, R. A. Botros, and D. Ceglarek, "Closed-loop gap bridging control for remote laser welding of aluminum components based on first principle energy and mass balance," J. Laser Appl. **31**, 022416 (2019).

Meet the Authors

Dr Mikhail Sokolov is a research fellow at Warwick Manufacturing Group (WMG), University of Warwick. His focus is laser beam welding, remote laser welding, and methods for improving welding efficiency and in-process monitoring using OCT technology.

Dr Pasquale Franciosa is a associate professor at WMG, University of Warwick. His research focus is smart manufacturing, process monitoring, closed-loop quality control, machine learning, and multidisciplinary optimization, with specific attention to automotive assembly systems and laser joining technologies for both similar and dissimilar materials. Currently, he is head of the laser welding applications laboratory at WMG.

Dr Tianzhu Sun is a research fellow at University of Warwick. His research activities are focused on understanding relationships between microstructure and properties of light alloys in the application of laser welding and friction stir welding processes.

Professor Darek Ceglarek is EPSRC Star Recruit Research Chair, U-Warwick, and a CIRP Fellow. Previously, he was Professor in IS&E at U-Wisconsin-Madison. He received his Ph.D. in ME, U-Michigan-Ann Arbor (1994). He focuses on smart manufacturing, data mining/AI for root cause analysis across design, manufacturing and service. He has been PI/co-PI on research grants of over £30M: NSF/NIST/EPSRC/InnovateUK/APC/EU-FP7/Marie Curie and industry. He has published over 180 papers, is listed by Stanford University among Top 2% of the world's leading scientists; received several Best Paper Awards; 2018 JLR "Innovista" Award for the most innovative "piloted technology"; EPSRC Star Award, NSF CAREER Award. He has served as AEs: ASTM SSMS; IEEE TASE, and ASME JMSE.

Vincenzo Dimatteo is a Ph.D. student in the department of Industrial Engineering of the University of Bologna; his research work focuses on laser welding of high-reflective materials for the manufacturing of electric powertrain components in the automotive industry.

Dr Alessandro Ascari is assistant professor at the University of Bologna, Italy. He has been dealing with industrial laser processes since 2005 and his research activity ranged among high power welding, surface transformation hardening, welding of dissimilar and cellular materials, cladding and cutting.

Dr Alessandro Fortunato is an associate professor at the University of Bologna. His current topics include laser materials processing, laser manufacturing through additive manufacturing and laser-matter interactions with ultrashort pulses. He is the coordinator of the Centre of Advanced Laser Manufacturing at the University of Bologna.

Falk Nagel obtained M.Sc. at the Technische Universität Ilmenau (Germany) and is employed as an application engineer at Coherent (Deutschland) GmbH.